

Unilamellar Vesicles as Potential Capreomycin Sulfate Carriers: Preparation and Physicochemical Characterization

Submitted: July 17, 2003; Accepted: October 23, 2003

Stefano Giovagnoli,¹ Paolo Blasi,¹ Claudia Vescovi,¹ Giuseppe Fardella,¹ Ione Chiappini,¹ Luana Perioli,¹ Maurizio Ricci,¹ and Carlo Rossi¹

¹Department of Chemistry and Technology of Drugs, Università degli Studi di Perugia, Via del Liceo 1, 06123 Perugia, Italy

ABSTRACT

The aim of this work was to evaluate unilamellar liposomes as new potential capreomycin sulfate (CS) delivery systems for future pulmonary targeting by aerosol administration. Dipalmitoylphosphatidylcholine, hydrogenated phosphatidylcholine, and distearoylphosphatidylcholine were used for liposome preparation. Peptide-membrane interaction was investigated by differential scanning calorimetry (DSC) and attenuated total internal reflection Fourier-transform infrared spectroscopy (ATR-FTIR). Peptide entrapment, size, and morphology were evaluated by UV spectrophotometry, photocalorimetry, and transmission electron microscopy, respectively. Interaction between CS and the outer region of the bilayer was revealed by DSC and ATR-FTIR. DSPC liposomes showed enhanced interdigitation when the CS molar fraction was increased. Formation of a second phase on the bilayer surface was observed. From kinetic and permeability studies, CS loaded DSPC liposomes resulted more stable if compared to DPPC and HPC over the period of time investigated. The amount of entrapped peptide oscillated between 10% and 13%. Vesicles showed a narrow size distribution, from 138 to 166 nm, and a good morphology. These systems, in particular DSPC liposomes, could represent promising carriers for this peptide.

KEYWORDS: capreomycin sulfate, liposomes, DSC, ATR-FTIR, phase transition

INTRODUCTION

After a century of decline, in the past decade a worrying recrudescence of tuberculosis (TB) has been observed.

This increasing incidence of TB is attributable to several factors, the most important of which are the HIV epidemic and the lack of control of immigration from countries where TB is common. In fact, untreated HIV infection, leading to progressive immunodeficiency, increases susceptibility to TB, one of the main causes of death in populations with high HIV prevalence.¹⁻³

The lack of DOTS (directly observed treatment short course), the strategy for TB control promoted by the World Health Organization, together with the improper use of antibiotics in chemotherapy are the main causes of the alarming multidrug resistance of new emerging strains to the most commonly used antitubercular drugs, such as ethambutol, isoniazid, rifampicin and streptomycin. Drug-resistant TB is treatable, but it requires extensive chemotherapy (up to 2 years of treatment) that is often prohibitively expensive and very toxic to patients.

In these cases, the less common and generally more toxic second- and third-line drugs such as p-aminosalicylic acid (PAS), capreomycin, cycloserine, ethionamide, kanamycin, and viomycin must be employed alone or in combination.

In this regard, the development of new effective agents and/or alternative formulations for drugs already existing in the market is necessary.

Improvement of the efficacy of antimicrobial agents against microorganisms located inside cells has been achieved by drug entrapment within liposomes. In fact, most antibiotics are relatively ineffective for intracellular infections because of poor penetration into the cells or decreased intracellular activity. In this respect, the development of proper liposome formulations may enhance antimicrobial treatment of intracellular infections,⁴ such as tuberculosis,^{5,6} and simultaneously reduce the toxicity of second-line antitubercular drugs such as capreomycin sulfate (CS).⁷

CS is a highly water-soluble peptide characterized by 4 co-existing cyclic forms. It is used, intramuscularly (15-20 mg/kg/day), in combination with other effective drugs, in the treatment of tuberculosis that has failed to respond to first-line agents.⁸ It is active in vitro and in vivo against *Mycobacterium tuberculosis*, *M bovis*, *M kansasii*, and *M*

Corresponding Author: Carlo Rossi, Department of Chemistry and Technology of Drugs, Università degli Studi di Perugia, 06123 Perugia, Italy;
Tel: +39-075-5855127; Fax: +39-075-5855163;
Email: cfrossi@unipg.it

avium. Resistance develops readily when capreomycin is used alone. Cross-resistance between capreomycin and viomycin, and partial cross-resistance between capreomycin and kanamycin or neomycin, have been demonstrated.⁸ Recently, the Italian National Institute of Health (ISS) showed that, among second-line antitubercular drugs, only about 10% of the 46 drug-resistant strains of *M tuberculosis* isolated from Italian patients were resistant to capreomycin.⁹

To overcome CS's toxic effects on kidneys, site-specific delivery systems can be employed. In particular, it has been demonstrated that entrapment of CS in multilamellar vesicles (MLVs) reduced renal toxicity, enhanced peptide penetration into tissues, and increased CS activity in a beige mouse model of *M avium* complex infection.⁷

Pulmonary administration of aerosolized liposomes represents a valid alternative route for topical drug delivery for lung infection treatments.¹⁰⁻¹⁴ The advantages of such an administration route are (1) facilitated administration of sustained-release formulations to maintain therapeutic drug levels in the lungs, (2) aqueous compatibility, and (3) facilitated intracellular delivery, particularly to alveolar macrophages and lymphocytes.¹³⁻¹⁵ Moreover, aerosol inhalation is a noninvasive means of delivery for peptides and proteins.¹⁶ This noninvasiveness allows the improvement of patient compliance. Looking at this alternative therapeutic application and considering the remarkable *in vivo* results,⁷ we investigated large unilamellar vesicles (LUVs) as potential CS carriers for possible peptide pulmonary delivery. In fact, LUVs may be more suitable for this particular application because, compared with MLVs, they are smaller and their size can be better controlled and homogenized.¹⁷ In fact, LUV size can be regulated by choosing extruding membranes having an appropriate cutoff.

Therefore, the aim of this study was the physicochemical characterization of LUVs in order to assess their suitability as CS carriers for peptide delivery. In this regard, 3 liposome-based formulations—dipalmitoylphosphatidylcholine (DPPC), hydrogenated phosphatidylcholine (HPC), and distearoylphosphatidylcholine (DSPC)—containing increasing CS molar fractions were prepared. All formulations were characterized in terms of their thermotropic behavior as a function of CS concentration and time, morphology, peptide encapsulation, and size. For this purpose, gel to liquid-crystal membrane main transition, stability, and membrane permeability to CS were evaluated by differential scanning calorimetry (DSC). Moreover, peptide encapsulation was determined by UV spectrophotometry, liposome size distribution was assessed by photocorrelation spectroscopy, and morphology was assessed by transmission electron microscopy (TEM). Further spectroscopic analyses were performed by attenuated total internal reflection Fou-

rier-transform infrared (ATR-FTIR) spectroscopy as a method complementary to DSC analysis.

MATERIALS AND METHODS

Materials

CS from *Streptomyces capreolus* and DPPC, HPC, and DSPC phospholipids were purchased from Sigma Aldrich Chemical (Milan, Italy). Sodium hydrogen orthophosphate was provided by Farmitalia Carlo Erba (Milan, Italy) and chloroform by J. T. Baker (Milan, Italy). Poly-L-lysine, phosphotungstic acid, and Triton X-100 reduced form were purchased from Sigma Aldrich. Ultrapure water was obtained by reverse osmosis through a Milli-Q system (Millipore, Rome, Italy). All other reagents and solvents were of the highest purity available.

Liposome Preparation

Three batches for each liposome formulation were prepared according to the thin-layer evaporation method. Briefly, thin lipid films were obtained by dissolving 25 mg of DPPC, HPC, and DSPC in chloroform followed by solvent evaporation under nitrogen stream on a water bath at 52°C, 61°C, and 65°C, respectively. The dry films were hydrated with proper amounts of pure phosphate buffer saline (PBS) (pH 7.4) and PBS solutions, yielding increasing peptide molar fractions ($\alpha = 0.06, 0.08, 0.10, 0.12, 0.14, 0.16, 0.18$), and the final sample volume was chosen to achieve 20mM lipid concentration. After cooling, the MLV suspensions were stored overnight at 4°C. LUVs were obtained by extruding (20 passes) MLV dispersions through a 0.1- μm pore size polycarbonate filter (Avestin Inc, Ottawa, Canada) mounted on a LiposoFast mini-extruder (Avestin Inc) at the same operating temperatures employed during the hydration process.¹⁸ The samples obtained were allowed to stabilize for 24 hours at 4°C.

Evaluation of CS Loading

The amount of peptide encapsulated was evaluated by UV spectrophotometry using a UV/Visible Jasco N-520 spectrophotometer (Jasco Inc, Easton, MD). Liposome suspensions were properly ultracentrifuged (70 000 rpm, 2 hours, 4°C) by an Optima TL ultracentrifuge equipped with a TLA-100.4 rotor (Beckman, Palo Alto, CA). Supernatant aliquots were directly analyzed by measuring CS absorbance at 268 nm. The entrapped CS within the unilamellar vesicles was determined after resuspension of the pellets in PBS buffer pH 7.4 and addition of 10% reduced Triton X-100 solution according to the method already described.¹⁹

Accordingly, total CS concentration of the 3 LUV formulations was determined on freshly prepared suspensions, and the error was calculated as SD. All measurements were performed in triplicate.

Size Distribution and Morphology

Size distribution of CS containing LUVs and blank LUVs was determined by a Nicomp 370 (PSS Inc, Santa Barbara, CA) autocorrelator equipped with a Coherent Innova 70-3 (Laser Innovations, Moorpark, CA) argon ion laser. The source was set at 514.5 nm. All analyses were performed at a 90° scattering angle and at 20°C (±0.2°C). Triplicate samples for each batch were prepared by diluting 10 µL of liposome suspension with 2 mL of deionized water filtered with an Acrodisc LC 13 Polyvinylidene fluoride (PVDF) filter with 0.2-µm pores (Pall-Gelman Laboratories, Ann Arbor, MI). The error was calculated as SD.

Morphology was performed by TEM using a Philips XL30 microscope at ×60 000 magnification. Samples were prepared by the method described elsewhere²⁰ on a Formvar-coated copper grid (TAAB Laboratories Equipment Ltd, Reading, UK) made hydrophilic by using poly-L-lysine. Phosphotungstic acid was employed as a negative stain.

DSC Measurements

DSC experiments were performed by a Mettler Toledo DSC 821 differential calorimeter (Milan, Italy) calibrated with indium. The detection system was a Mettler PT 100 ceramic sensor, with a calorimetric resolution <0.7 µW and noise level <1 µW. The analyses were carried out on 40-µL samples, corresponding to ~1.0 mg of lipid material sealed in standard aluminum pans (Mettler Toledo, Milan, Italy). Three samples per LUV batch were submitted to 2 heating/cooling cycles at 1°C min⁻¹. Isotonic PBS buffer (pH 7.4) was employed as reference. Data from the first scan were always discarded to avoid mixing artifacts. Control samples consisted of CS-free phospholipid vesicle suspensions. Enthalpy change (ΔH), main transition peak temperature (T_m), and half-height peak widths (ΔW_{1/2}) were calculated by Mettler Toledo STARE software version 6.01. Mathematical curve fitting of the main transition peak was performed by SYSTAT's Peakfit v. 4.11 software (Canal Boulevard, Richmond, CA, USA).

Kinetic Interaction Studies

CS-loaded LUV samples were incubated for 14 days at 4°C, under nitrogen atmosphere. Aliquots (40 µL) were periodically withdrawn and submitted to DSC analysis. As a consequence of the thermal perturbation of the system, only the

first heating scan was considered. Each set of measurements was accompanied by a control sample made of pure liposomes. For permeability study, CS-free LUVs were prepared as previously described and ultracentrifuged at 70 000 rpm for 30 minutes. The pellets were resuspended in CS PBS solution pH 7.4 and incubated at 25°C for 48 hours and 4°C for 9 days. Aliquots (40 µL) were periodically withdrawn and submitted to DSC analysis. All samples were maintained under nitrogen atmosphere to prevent oxidation.

ATIR-FTIR Analysis

Infrared spectroscopy experiments were carried out by a Jasco FT/IR-410 (Lecco, Italy) spectrometer equipped with a deuterated, L-alanine doped triglycine sulfate detector and a Potassium Bromide (KBr) beam splitter. Exactly 100 µL of DPPC, HPC, and DSPC LUV samples (~200 mg phospholipids) were prepared as already described elsewhere²¹ on a 75 × 10 × 2 mm, θ = 45°, n = 2.24, Zinc Selenide (ZnSe) crystal (PIKE Technologies, Madison, WI), yielding 12 internal reflections. This procedure was performed in triplicate. Reference samples consisted of blank liposomes, and the background medium was PBS pH 7.4. All measurements were performed at room temperature in the 3800 to 800 cm⁻¹ wavelength range. For each spectrum, 256 interferograms were collected at 2 cm⁻¹ resolution. The curves were deconvoluted and imported in SYSTAT's Peakfit v. 4.11 software, and Gaussian curve fitting was performed.

RESULTS AND DISCUSSION

Peptide Loading

Spectrophotometric analysis of liposomes highlighted that similar quantities of peptide were encapsulated in all phospholipid vesicles (**Table 1**). The CS amount entrapped oscillated between 10% and 13% of the total peptide. The low value found for these vesicles is, perhaps, due to the high hydrophilicity of the peptide that readily diffuses in the outer aqueous solution.

Size Distribution and Morphology

CS-loaded LUV size distribution resulted homogeneous, sharp and with a polydispersion <40%. The mean diameter was 138, 158, and 166 nm for DPPC, HPC, and DSPC vesicles, respectively (**Table 1**). Blank liposomes did not show any modification with respect to loaded LUVs, and their mean diameter was around 150 nm (data not shown). TEM pictures revealed good homogeneity and uniformity of liposome suspensions (**Figure 1**).

Table 1. Entrapped Peptide Within HPC, DPPC, and DSPC Liposomes*

Liposomes [†]	Entrapped Peptide \pm SD (%) [‡]	Mean Diameter \pm SD (nm)
HPC	13 \pm 3	158 \pm 30
DPPC	10 \pm 1	138 \pm 35
DSPC	10 \pm 3	166 \pm 40

*The encapsulation is expressed as the amount found in the pellet with respect to the total amount calculated from the freshly prepared suspension. The CS molar fraction was 0.16.

CS indicates capreomycin sulfate; DPPC, dipalmitoylphosphatidylcholine; DSPC, distearoylphosphatidylcholine; HPC, hydrogenated phosphatidylcholine.

[†]0.16 molar fraction.

[‡](CS in the pellets/total CS amount in the suspension) x 100.

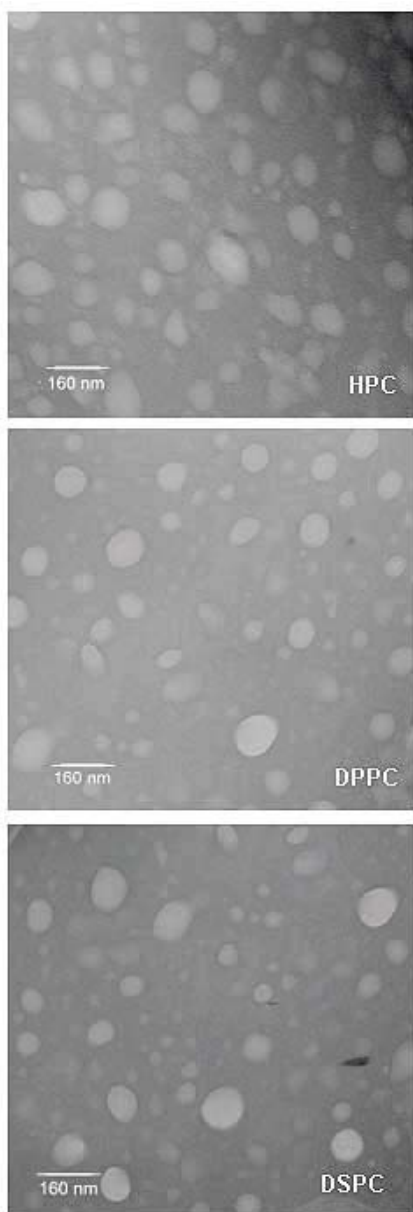


Figure 1. TEM pictures of CS-loaded liposomes. Magnification was $\times 60\,000$. Dimensional bars are reported as well.

DSC Analysis

It is well known that foreign molecule interactions with bilayer ordered structures can influence the thermotropic behavior of a pure liposome system in conformity with their own physicochemical properties.^{22,23} Consequently, CS loading in pure phospholipid bilayers may change the $P\beta \rightarrow L\alpha$ gel to liquid crystalline main transition profile. DSC analyses on DPPC, HPC, and DSPC LUVs pointed out the acyl chain length effect on CS-loaded vesicle thermotropic behavior. The results showed no change of the transition temperatures investigated (**Table 2**). This behavior is typical of very hydrophilic compounds, such as CS, which because of their physicochemical properties hardly penetrate the lipid surface. Moreover, the $L\beta \rightarrow P\beta$ gel to “ripple” phase pretransition, present in empty DPPC or DSPC LUVs, disappeared completely even at the lowest CS α values (**Figure 2**). Pure HPC liposomes did not show any pretransition because of their lower chain order. Slight broadening of DPPC and HPC main transition peaks was observed as well (**Table 2**). The enhanced effect observed for HPC is probably due to its heterogeneous structure, as indicated by a much broader peak of the pure bilayers with respect to DPPC and DSPC vesicles. The presence of different acyl chains, such as palmitic and stearic, in HPC bilayers, although increasing the packing energies (as shown by a higher chain melting temperature for HPC than DPPC), reduces the cooperation in the hydrophobic chain region. In fact, HPC vesicles showed a lower transition enthalpy as a consequence of a decreased acyl chain order. The effect of this decreased order in the hydrophobic region is an enhanced susceptibility to CS loading, resulting in a more accentuated broadening at increased α values (**Table 2**). The same considerations may be valid for CS-DPPC vesicles, but in this system the remarkably higher palmitic chain order resulted in a smaller decrease in cooperation that reflects higher enthalpy values and smaller broadening of the main transition peak. Tighter acyl chain aggregation was observed at $\alpha = 0.08$. This effect was due to the acyl chain interdigitation, which remarkably decreased $\Delta W_{1/2}$ and increased the enthalpy value. When

Table 2. DPPC, HPC, and DSPC Vesicle DSC Parameters as Function of CS Molar Fraction*

CS Molar Fraction	T _m (°C)† ± SD	ΔH _T (kcal/mol) ± SD	ΔW _{1/2} (°C)‡ ± SD
<i>DPPC</i>			
0.00	40.69 ± 0.01	7.40 ± 0.06	0.830 ± 0.006
0.06	40.71 ± 0.05	6.63 ± 0.16	0.903 ± 0.006
0.08	40.67 ± 0.02	7.62 ± 0.16	0.533 ± 0.010
0.10	40.71 ± 0.02	6.88 ± 0.20	0.800 ± 0.010
0.12	40.78 ± 0.03	6.67 ± 0.22	0.807 ± 0.010
0.14	40.76 ± 0.02	6.66 ± 0.21	0.880 ± 0.010
0.16	40.81 ± 0.04	6.64 ± 0.06	0.943 ± 0.006
0.18	40.77 ± 0.03	6.63 ± 0.18	1.047 ± 0.006
<i>HPC</i>			
0.00	50.34 ± 0.03	6.27 ± 0.10	2.67 ± 0.05
0.06	50.66 ± 0.06	6.10 ± 0.32	2.87 ± 0.03
0.08	50.26 ± 0.04	6.08 ± 0.13	2.88 ± 0.02
0.10	50.63 ± 0.02	6.06 ± 0.13	2.95 ± 0.05
0.12	50.69 ± 0.10	5.98 ± 0.11	3.02 ± 0.06
0.14	50.65 ± 0.15	5.89 ± 0.06	3.17 ± 0.03
0.16	50.62 ± 0.13	5.60 ± 0.04	3.14 ± 0.09
0.18	50.79 ± 0.09	5.71 ± 0.07	3.11 ± 0.01
<i>DSPC</i>			
0.00	55.08 ± 0.01	7.42 ± 0.10	0.77 ± 0.02
0.06	55.13 ± 0.04	6.62 ± 0.14	0.84 ± 0.01
0.08	55.09 ± 0.03	6.79 ± 0.09	0.83 ± 0.01
0.10	55.10 ± 0.02	6.93 ± 0.15	0.81 ± 0.01
0.12	54.99 ± 0.05	6.94 ± 0.01	0.77 ± 0.01
0.14	55.10 ± 0.03	6.98 ± 0.13	0.71 ± 0.01
0.16	55.09 ± 0.04	7.00 ± 0.13	0.70 ± 0.02
0.18	55.06 ± 0.03	7.42 ± 0.09	0.63 ± 0.01

*All parameters refer to the transition peak of the second DSC scan in heating mode; the values are the average of 3 different experiments. CS indicates capreomycin sulfate; DPPC, dipalmitoylphosphatidylcholine; DSC, differential scanning calorimetry; DSPC, distearoylphosphatidylcholine; HPC, hydrogenated phosphatidylcholine.

†Main transition peak temperature.

‡Width half-height of the main transition peak of the bilayers.

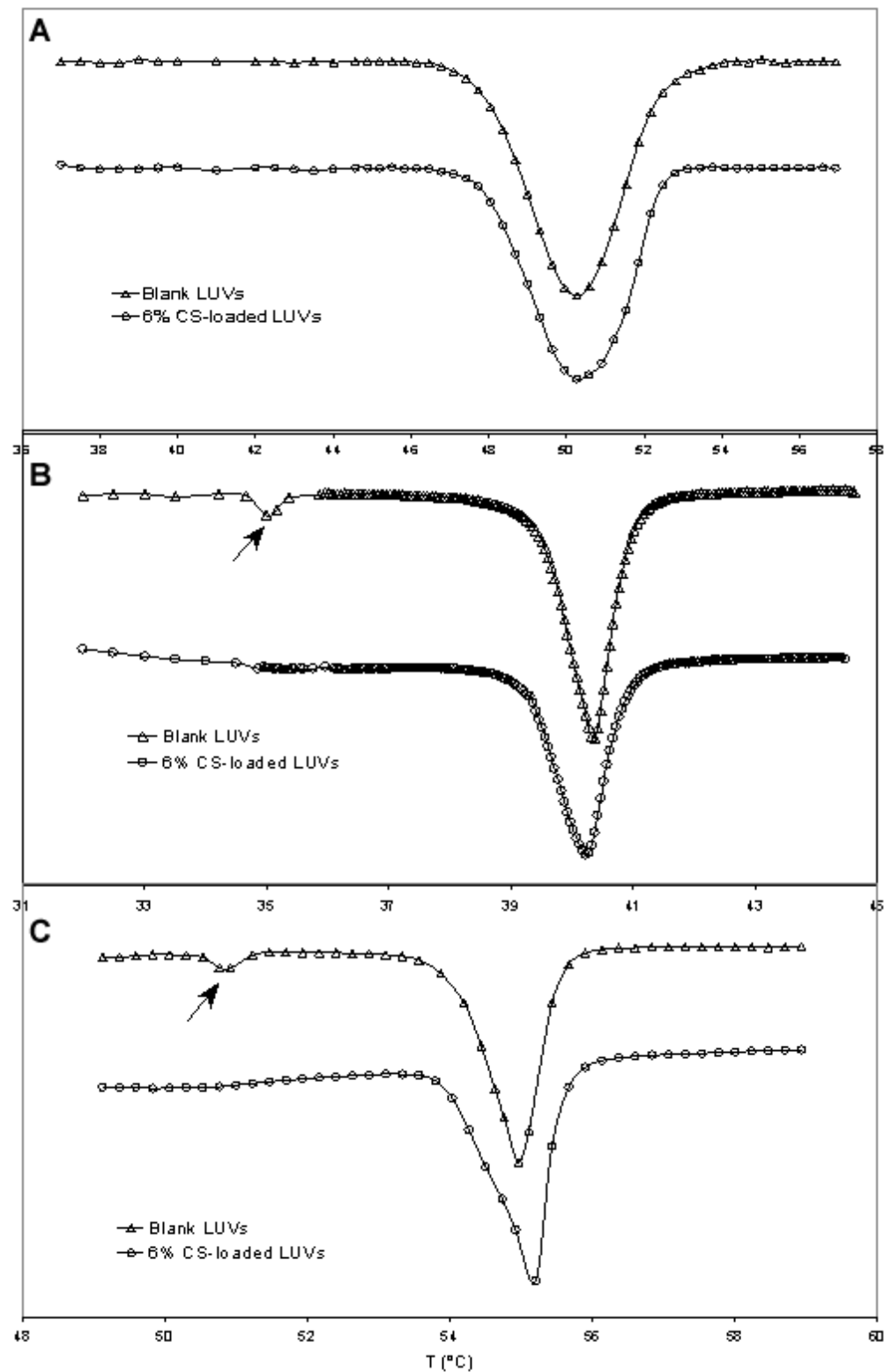


Figure 2. (A) HPC, (B) DPPC, and (C) DSPC LUV thermograms showing the disappearance of pretransition after CS loading. The pretransition peaks are indicated by an arrow. Pure HPC liposomes did not show any pretransition peak, as a result of their lower chain order.

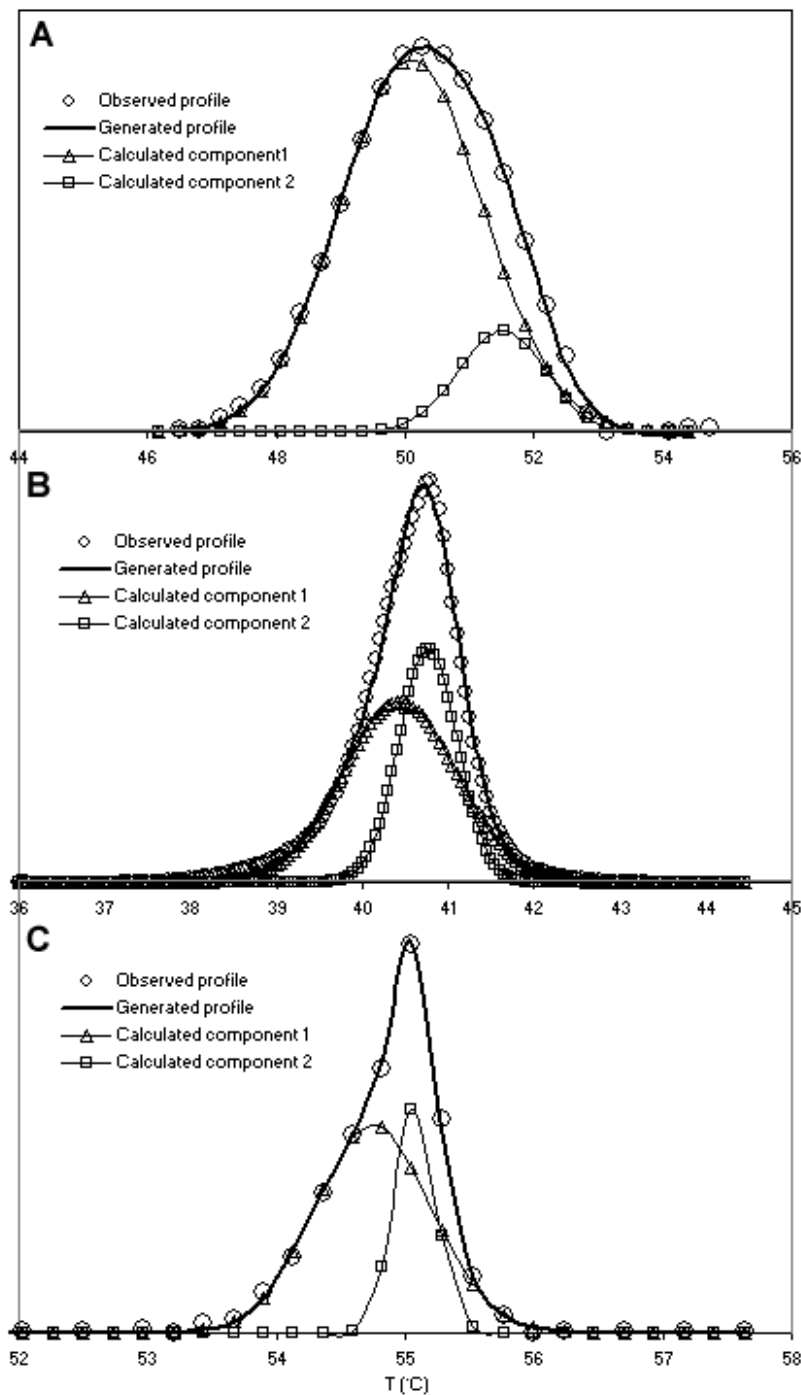


Figure 3. Mathematical calculation of the main transition peak components: (A) 0.18 molar fraction CS-loaded HPC vesicles; (B) 0.18 molar fraction CS-loaded DPPC vesicles; (C) 0.18 molar fraction CS-loaded DSPC vesicles. Correlation was >0.990 . It is evident that there was a second component, calculated at 50.08°C, 40.50°C, and 54.76°C, for HPC, DPPC, and DSPC, respectively. In spite of the presence of the second component, DSPC showed a different behavior with narrower peaks at higher CS concentration because of interdigitation.

Table 3. Calculated Data for HPC, DPPC, and DSPC Liposomes Containing CS*

r^2	HPC		DPPC		DSPC	
	0.99861		0.99736		0.99916	
Peak	Peak Center \pm SD	% Area \pm SD	Peak Center \pm SD	% Area \pm SD	Peak Center \pm SD	% Area \pm SD
1	51.49 \pm 0.05	15 \pm 7	40.81 \pm 0.05	35 \pm 8	55.09 \pm 0.04	28 \pm 3
2	50.08 \pm 0.10	85 \pm 7	40.50 \pm 0.07	65 \pm 8	54.76 \pm 0.07	72 \pm 3

*CS indicates capreomycin sulfate; DPPC, dipalmitoylphosphatidylcholine; DSPC, distearoylphosphatidylcholine; HPC, hydrogenated phosphatidylcholine.

$\alpha > 0.08$, DPPC vesicles lost the enhanced order and either enthalpies begin to decrease or peaks begin to broaden. DSPC LUVs, except for the already mentioned effect on the transition temperature, showed a completely different behavior than did DPPC and HPC formulations. The results showed a progressive enthalpy increment that, at the highest α values, matched the value of the pure DSPC vesicles. After an initial broadening at $\alpha = 0.06$, sharpening of the peaks was observed with the increase of α values. These findings are the result of a progressive acyl chain interdigitation as confirmed by the continuous decrease of $\Delta W_{1/2}$ with the increase of CS concentration (Table 2). Mathematical fitting of the main transition peak, performed on $\alpha = 0.18$ samples (Figure 3), highlighted the presence of a second component. This new peak represents an outer CS-rich segregation phase that allows phospholipids to melt differently from the CS-poorer hydrophilic portions of the bilayer, generating an asymmetric transition peak profile. The fitting process resulted in a correlation > 0.99 and a standard error < 0.008 (Table 3). The calculated second component was at 50.08°C, 54.76°C, and 40.50°C for HPC, DSPC, and DPPC, respectively. The high percent area of the second component for DSPC (72%) shows the correlation between the interdigitation increase and the accumulation of CS on the outer surface of the bilayer (Table 3).

Kinetic Study: Permeability and Stability

DSC scans of DPPC, HPC, and DSPC LUVs did not present particular modifications on Tm trend profiles, whatever the α value, indicating that no CS penetration occurred in the phospholipid bilayer throughout the period investigated. ΔH and $\Delta W_{1/2}$ do not seem to change significantly either, especially when compared to the data obtained from the control samples consisting of pure liposome preparations. These findings suggest that no degradation or relevant interaction changes affected the CS-loaded vesicles during 14 days of incubation at 4°C and that these systems seem to behave in a way that is not dependent on CS loading. A confirmation of these results was obtained from permeability studies (Figure 4). When the transition peak profiles of DPPC, HPC, and DSPC dispersed in a CS solution were

compared, no changes were pointed out in peak shapes and no Tm shifts were observed. As expected, the interaction is limited to the outer region of the bilayer without involving hydrophobic chains that are influenced only peripherally by the forces acting on the polar headgroups. Moreover, these results suggest that the amount of drug interacting with the bilayer is constant with time because, otherwise, changes in vesicle thermal profiles would be observed.

FTIR Analysis

ATR-FTIR is one of the most powerful techniques for performing IR spectra of lipids and peptides or proteins, since it allows the simultaneous analysis of their structure and, moreover, can provide very reliable data on highly aggregated materials and large membrane fragments.²⁴ Analyses were accomplished on phospholipid C=O, C-H, and PO₂ stretching bands. Measurements performed on pure and CS-loaded LUVs confirmed the presence of phospholipid carboxylic group stretching at 1735 cm⁻¹ for pure HPC and DSPC, and at 1736 cm⁻¹ for pure DPPC, within the range of 1742 to 1725 cm⁻¹ elsewhere proposed.²⁴⁻²⁶ The overlapped second band appearing in CS-loaded vesicle spectra (Figure 5), in the range 1667 to 1706 cm⁻¹, corresponds to the amide I absorption of the peptide.²⁷

Mathematical curve fitting (Table 4) pointed out that CS loading caused a decrease (approximately -4 cm⁻¹) in HPC vesicles' C=O stretching, whereas DSPC and DPPC LUVs showed modifications within the experimental error. The shift observed is the consequence of possible hydrogen bonding on the carboxylic group due to the presence of water²⁸ as confirmed by the peak broadening (7 cm⁻¹). These effects show that HPC LUVs are more susceptible to CS loading. In turn, the C-H stretching was less influenced by the peptide loading, showing variations within the experimental error.

Analysis of PO₂ antisymmetric and symmetric stretching showed main absorption at approximately 1242 to 1245 cm⁻¹, and 1085 to 1094 cm⁻¹, respectively, within the range of 1220 to 1250 cm⁻¹ and 1085 to 1100 cm⁻¹ proposed else

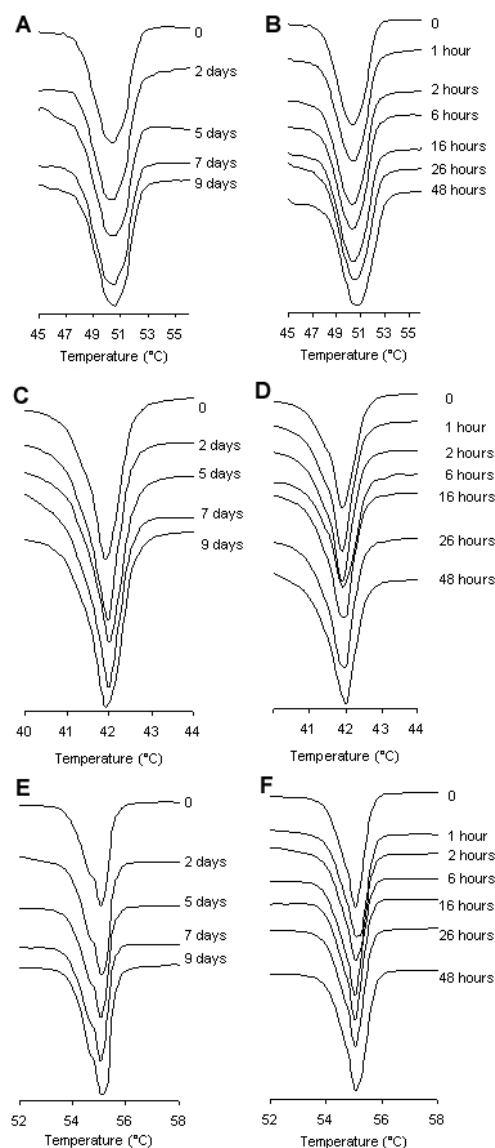


Figure 4. Permeability study for CS-HPC system performed at (A) 4°C and (B) 25°C; permeability study for CS-DPPC system performed at (C) 4°C and (D) 25°C; and permeability study for CS-DSPC system performed at (E) 4°C and (F) 25°C.

where.²⁴⁻²⁶ The mathematical fitting revealed shift (approximately -3 cm^{-1}) and broadening (approximately 16 cm^{-1}) for DSPC symmetric and for DPPC antisymmetric stretching (approximately 5 cm^{-1}) (Table 5). These findings correlate well with the conformational change pointed out by comparison of pure and loaded LUV profiles (Figure 6). The remarkable difference between pure and loaded DSPC LUVs (Figure 6C), if compared to the other phospholipids, resembles what was found in the DSC study.

Three important conclusions can thus be inferred: (1) polar headgroups are the main CS interaction sites, (2) the HPC

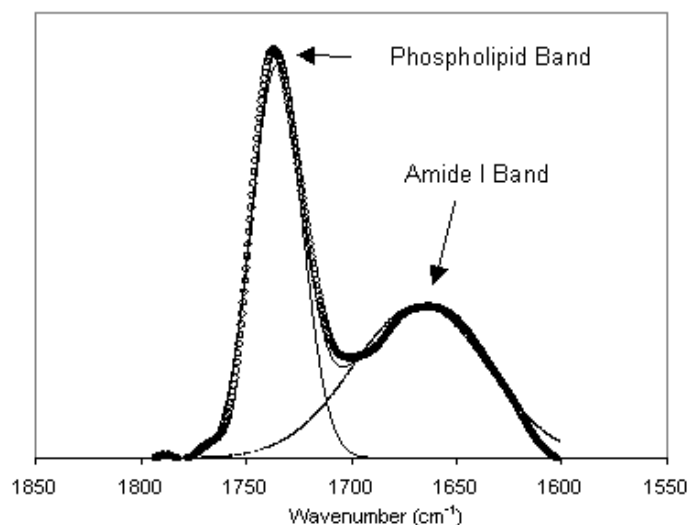


Figure 5. CS-loaded liposome profiles in the carbonyl stretching region showing the presence of the amide I component of the peptide. The main bands are indicated.

system was the most sensitive to CS loading and 3) the DSPC conformational modifications observed by FTIR between pure and loaded LUVs were due to the acyl chain interdigitation induced by CS loading. These observations match DSC findings, which also featured interdigitation of CS loaded DSPC bilayers and HPC LUVs higher sensitivity to CS loading.

CONCLUSION

The present study revealed differences in the behavior of DSPC, DPPC, and HPC LUVs. DSC scans showed the enhanced stability of CS-loaded DSPC vesicles, because of induced interdigitation of the stearic acyl chains. These results, confirmed by IR measurements, demonstrated that DSPC may represent a more suitable phospholipid carrier for this peptide than DPPC and HPC do. The proved effectiveness in mice,⁷ the relative stability and homogeneity of these preparations (in particular, DSPC vesicles), and the CS activity against multidrug-resistant bacteria strains⁹ make these formulations worthy of being tested, after appropriate modification if needed, for a possible aerosol application.

ACKNOWLEDGEMENTS

This work was supported by the Italian Ministry for Education, University and Research—research programs of national interest. Special thanks are due to Professor Patrick P. DeLuca of the University of Kentucky, Lexington, Kentucky, who kindly placed at our disposal the mathematical fitting software.

Table 4. Shifts and Bandwidths of the Main Functional Group Bands for Blank and CS-Loaded Liposomes*

Bands	Blank Liposomes		CS-Loaded Liposomes ($\alpha=0.16$)	
	Peak Center (cm^{-1}) \pm SD	Bandwidth (cm^{-1}) \pm SD	Peak Center (cm^{-1}) \pm SD	Bandwidth (cm^{-1}) \pm SD
<i>HPC</i>				
Antisymmetric C-H stretching	2917.60 \pm 0.04	14.53 \pm 0.15	2917.64 \pm 0.05	16.05 \pm 0.23
Symmetric C-H stretching	2849.63 \pm 0.02	12.18 \pm 0.12	2849.68 \pm 0.01	14.20 \pm 0.45
C=O stretching	1739.55 \pm 0.08	21.39 \pm 0.24	1736.29 \pm 0.07	27.64 \pm 0.63
<i>DPPC</i>				
Antisymmetric C-H stretching	2917.60 \pm 0.04	15.60 \pm 0.23	2917.75 \pm 0.06	15.47 \pm 0.42
Symmetric C-H stretching	2849.85 \pm 0.07	13.72 \pm 0.56	2849.92 \pm 0.08	13.77 \pm 0.33
C=O stretching	1734.42 \pm 0.06	28.41 \pm 0.42	1735.47 \pm 0.04	34.43 \pm 0.15
<i>DSPC</i>				
Antisymmetric C-H stretching	2917.25 \pm 0.06	15.22 \pm 0.11	2917.01 \pm 0.15	15.82 \pm 0.65
Symmetric C-H stretching	2849.60 \pm 0.02	13.59 \pm 0.10	2849.35 \pm 0.09	13.75 \pm 0.14
C=O stretching	1734.64 \pm 0.04	28.83 \pm 0.27	1734.52 \pm 0.03	29.56 \pm 0.49

*CS indicates capreomycin sulfate; DPPC, dipalmitoylphosphatidylcholine; DSPC, distearoylphosphatidylcholine; HPC, hydrogenated phosphatidylcholine.

Table 5. Calculated Antisymmetric and Symmetric PO₂ Stretching Data for Blank and CS-Loaded Liposomes*

Bands	Blank Liposomes		CS-Loaded Liposomes ($\alpha=0.16$)	
	Peak Center (cm^{-1}) \pm SD	Bandwidth (cm^{-1}) \pm SD	Peak Center (cm^{-1}) \pm SD	Bandwidth (cm^{-1}) \pm SD
<i>HPC</i>				
Antisymmetric PO ₂ stretching	1241.60 \pm 0.06	43.70 \pm 0.19	1242.94 \pm 0.05	46.44 \pm 0.16
Symmetric PO ₂ stretching	1094.63 \pm 0.08	45.60 \pm 0.22	1096.19 \pm 0.07	47.08 \pm 0.28
<i>DPPC</i>				
Antisymmetric PO ₂ stretching	1244.65 \pm 0.08	38.90 \pm 0.32	1241.58 \pm 0.03	43.91 \pm 0.25
Symmetric PO ₂ stretching	1085.05 \pm 0.05	54.27 \pm 0.45	1089.48 \pm 0.04	57.51 \pm 0.21
<i>DSPC</i>				
Antisymmetric PO ₂ stretching	1242.39 \pm 0.09	43.42 \pm 0.54	1243.18 \pm 0.08	45.81 \pm 0.11
Symmetric PO ₂ stretching	1093.01 \pm 0.04	36.73 \pm 0.14	1089.63 \pm 0.09	52.66 \pm 0.42

*CS indicates capreomycin sulfate; DPPC, dipalmitoylphosphatidylcholine; DSPC, distearoylphosphatidylcholine; HPC, hydrogenated phosphatidylcholine.

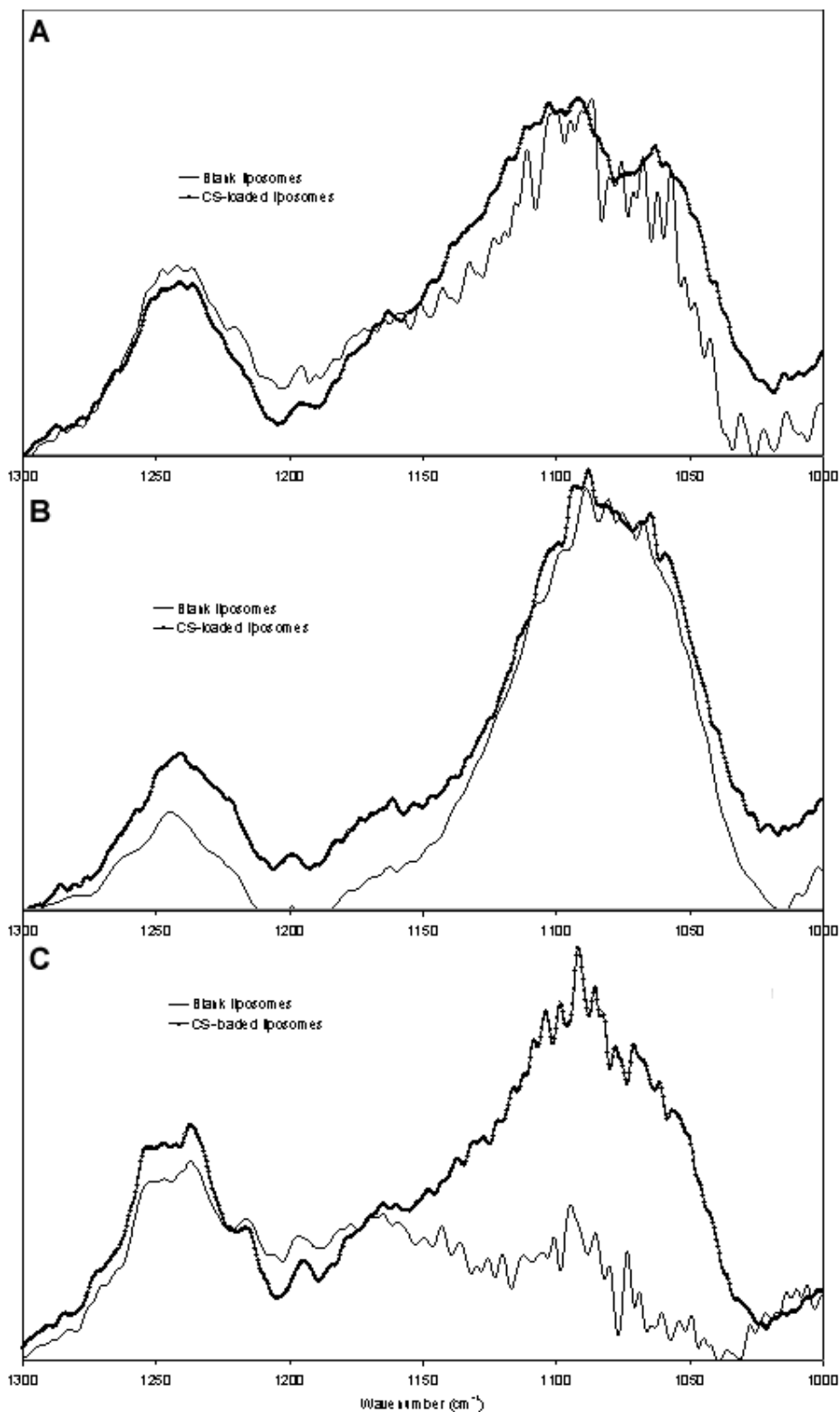


Figure 6. Blank and CS-loaded liposome profiles in the PO₂ stretching region for (A) HPC, (B) DPPC, (C) DSPC phospholipids. The effect on DSPC conformation points out the acyl chain interdigitation.

REFERENCES

1. Maher D, Floyd K, Raviglione M. A strategic framework to decrease the burden of TB/HIV. WHO report, World Health Organization/Communicable Diseases/Tuberculosis, 2002; 296.
2. Vigorita MG, Ottanà R, Zappalà C, Maccari R, Pizzimenti FC, Gabrielli G. Halogenated isoniazid derivatives as possible antimycobacterial and anti-HIV agents-III. *Il Farmaco*. 1994;49:775-781.
3. Ferrarini P, Manera C, Mori C, Badawneh M, Saccomanni G. Synthesis and evaluation of antimycobacterial activity of 4-phenyl-1,8-naphthyridine derivatives. *Il Farmaco*. 1999;53:741-746.
4. Gursoy A. Liposome-encapsulated antibiotics: Physicochemical and antibacterial properties, a review. *STP Pharma Sci*. 2000;10(4):285-291.
5. Deol P, Khuller GK. Lung specific stealth liposomes: stability, bio-distribution and toxicity of liposomal antitubercular drugs in mice. *Biochim Biophys Acta*. 1997;1334:161-172.
6. Pinto-Alphandary H, Andremont A, Couvreur P. Targeted delivery antibiotics using liposomes and nanoparticles: research and applications. *Int J Antimicrob Agents*. 2000;13:155-168.
7. Le Conte P, Le Gallou F, Potel G, Struillou L, Baron D, Drugeon HB. Pharmacokinetics, toxicity, and efficacy of liposomal capreomycin in disseminated *Mycobacterium avium* beige mouse model. *Antimicrob Agents Chemother*. 1994;38:2695-2701.
8. Martindale the Extra Pharmacopoeia. Capreomycin sulfate (7554-1). *The Complete Drug Reference—Monographs*. 32nd ed. Parfitt K editor, The Pharmaceutical Press, London, UK.; 1997:162.
9. Fattorini L, Iona E, Ricci ML, Thoresen OF, Orru G, Oggioni MR, Tortoli E, Piersimoni C, Chiaradonna P, Tronci M, Pozzi G, Orefici G. Activity of 16 antimicrobial agents against drug-resistant strains of *Mycobacterium tuberculosis*. *Microb Drug Resist*. 1999;5:265-270.
10. Farr SJ, Kellaway IW, Perry-Jones DR, Woolfrey SG. 99-m Technetium as a marker of liposomal deposition and clearance in the human lung. *Int J Pharm*. 1985;26:303-316.
11. Gilbert BE, Six HR, Wilson SZ, Wyde PR, Knight V. Small particle aerosols of enviroxime-containing liposomes. *J Antiviral Res*. 1988;9:355-365.
12. Niven RW, Schreier H. Nebulization of liposomes, I: effects of lipid composition. *Pharm Res*. 1990;7:1127-1133.
13. Schreier H, Gonzalez-Rothi RJ, Stecenko AA. Pulmonary delivery of liposomes. *J Control Release*. 1993;24:209-223.
14. Taylor KMG, Farr SJ. Liposomes for delivery to the respiratory tract. *Drug Dev Ind Pharm*. 1993;19:123-142.
15. Hung OR, Whynot SC, Varnel JR, Shafer SL, Mezel M. Pharmacokinetics of inhaled liposome encapsulated fentanyl. *Anesthesiology*. 1995;83:277-284.
16. Patton JS, Platz RM. Pulmonary delivery of peptides and proteins for systemic action. *Adv Drug Deliv Rev*. 1992;8:179-196.
17. Niven RW, Speer M, Schreier H. Nebulization of liposomes, II: the effects of size and modelling of solute release profiles. *Pharm Res*. 1991;8:2, 217-221.
18. Mayer LD, Hope MJ, Cullis PR. Vesicles of variable sizes produced by a rapid extrusion procedure. *Biochim Biophys Acta*. 1986;858:161-168.
19. Sivakumar PA, Panduranga KR. Development of stable polymerized vinyl-pyrrolidone cholesteryl methacrylate liposomes as carriers for drug delivery. *Biomed Microdev*. 2002;4:3, 197-204.
20. Moscho A, Orwar O, Chiu DT, Modi BP, Zare RN. Rapid preparation of giant unilamellar vesicles. *Proc Natl Acad Sci U S A*. 1996;93:11443-11447.
21. Goormaghtigh E, Raussens V, Ruyschaert JM. Attenuated total reflection infrared spectroscopy of proteins and lipids in biological membranes. *Biochim Biophys Acta*. 1999;1422:105-185.
22. Jain MK. Order and dynamics in bilayers and solute in bilayers. In: Jain MK, ed. *Introduction to Biological Membranes*. New York, NY: Wiley, 1988:122-165.
23. Taylor KMG, Morris RM. Thermal analysis of phase transition behaviour in liposomes. *Thermochim Acta*. 1995;248:289-301.
24. Weers JG, Scheuing DR. Characterization of viscoelastic surfactant mixtures, I: Fourier transform infrared spectroscopic studies. *Colloids Surf. B: Biointerfaces*, 1991;55:41-56.
25. Fringeli UP, Guenthard HH. Infrared membrane spectroscopy. *Mol Biol Biochem Biophys*. 1981;31:270-332.
26. Guenzler H, Boeck H. *IR Spectroscopy. An Introduction*. 2nd ed. Weinheim, Germany: Verlag Chemie; 1983:403. (In German)
27. Silvestro L, Axelsen PH. Infrared spectroscopy of supported lipid monolayer, bilayer, multibilayer membranes. *Chem Phys Lipids*. 1998;96:69-80.
28. Attar M, Wong PTT, Kates M, Carrier D, Jaklis P, Tanphaichitr N. Interaction between sulfogalactosylceramide and dimyristoylphosphatidylcholine increases the orientational fluctuation of their lipid hydrocarbon chains. *Chem Phys Lipids*. 1998;94:227-238.